



Article

Cationic Protic Imidazolylidene NHC Complexes of Cp^*IrCl^+ and Cp^*RhCl^+ with a Pyridyl Tether Formed at Ambient Temperature

Douglas B. Grotjahn ^{1,*}, Jessica K. Martin ¹, Taylon N. Tom ¹ and Arnold L. Rheingold ²

¹ Department of Chemistry and Biochemistry, San Diego State University, 5500 Campanile Drive, San Diego, CA 92182-1030, USA; jlamonte@gmail.com (J.K.M.); taylon219@yahoo.com (T.N.T.)

² Department of Chemistry and Biochemistry, University of California, San Diego, 9500 Gilman Drive, La Jolla, CA 92093-0385, USA; arheingold@ucsd.edu

* Correspondence: dbgrotjahn@mail.sdsu.edu; Tel.: +1-619-594-0231

Received: 16 January 2018; Accepted: 7 February 2018; Published: 14 February 2018

Abstract: Protic NHC (PNHC) complexes with N^1H , N^2 -alkyl/aryl imidazolylidene ligands are relatively rare, and routes for their synthesis differ from what is used to make non-protic analogs. Prior work from our group and others showed that in the presence of a tethering ligand (phosphine or in one case, pyridine), CpM and Cp^*M ($\text{M} = \text{Ir}, \text{Ru}$) PNHC complexes could be made by heating. Here, we find that the use of ionizing agents to activate $[\text{Cp}^*\text{M}^{\text{III}}\text{Cl}(\mu\text{-Cl})_2]$ ($\text{M} = \text{Ir}, \text{Rh}$) allows for what we believe is unprecedented ambient temperature formation of PNHC complexes from neutral imidazoles; the product complexes are able to perform transfer hydrogenation.

Keywords: iridium; rhodium; silver; *N*-heterocyclic carbene; protic; bifunctional; metalation; transfer hydrogenation

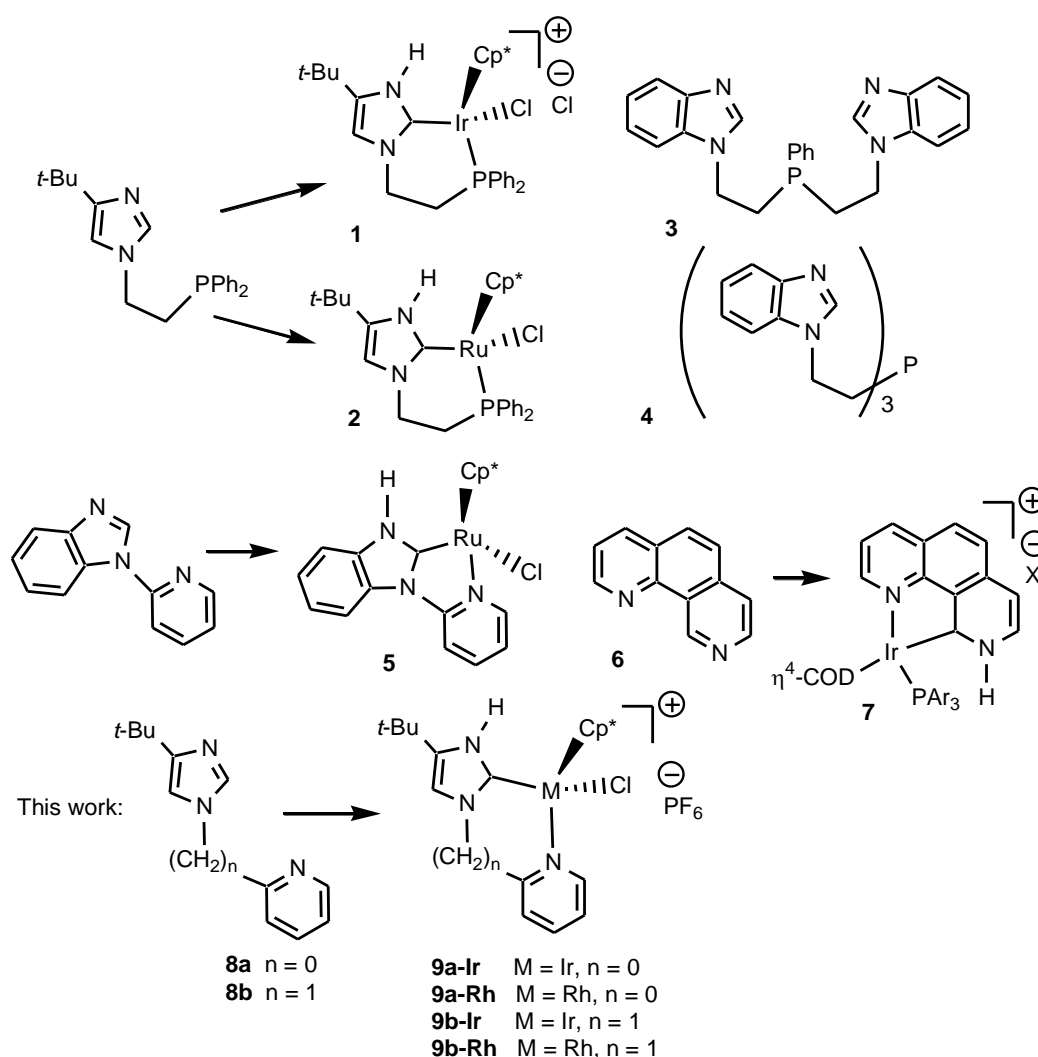
1. Introduction

The last 25 years have seen the establishment of *N*-heterocyclic carbenes (NHCs) as essential tools for creation of powerful metal-containing catalysts and organocatalysts. The predominant parent heterocycle that has been used is imidazole. The overwhelming majority of imidazolidene and imidazolylidene NHC ligands bear two non-hydrogen substituents on the ring nitrogens. By contrast, NH derivatives may be described as protic NHCs (PNHC) [1,2]. Whereas thousands of literature references describe NHCs, less than one hundred describe PNHCs, yet for PNHCs, there is the additional possibility of bifunctional chemistry and catalysis enabled by the protic functionality.

Synthetic routes to PNHC complexes must differ from those used to make NHC complexes. For example, in some syntheses of NHC complexes, free NHCs are made by deprotonating imidazolium salts; this route is precluded in making PNHCs, because the most acidic proton on the imidazolium salt precursor would be that on one of the nitrogens. Some PNHC complexes are made by coordination of a 1-alkylimidazole to a metal fragment, followed by deprotonation with the appropriate base at C-2, migration of the metal fragment to C-2, followed by protonation with the appropriate acid [3–5]. A variant on this scheme starts with C-2 deprotonation, installation of the metal at C-2, and protonation [6–8]. Occasionally, a suitable *N*-protecting group has been used [9]. All three of these routes involve three synthetic steps. Another route starts with a heterocycle functionalized at C2 with a halide; oxidative addition, followed by protonation afford PHNC complexes [10–12]. There is still a need for development of PNHC synthetic routes that are short and as general as possible.

To this end, our group and others have focused on developing reactions of 1-alkyl or 1-arylimidazole derivatives with a metal complex to form a N^1H , N^2 -alkyl/aryl PNHC complex in a single synthetic step, that most certainly happens by more than one mechanistic step in the same flask.

In 2008 and 2011, we reported the use of a 2-diphenylphosphinoethyl group as a tether to enable direct metalation by $[\text{Cp}^*\text{Ir}^{\text{III}}\text{Cl}(\mu\text{-Cl})_2]$ or $\text{Cp}^*\text{Ru}^{\text{II}}\text{Cl}(\text{COD})$ to form **1** and **2**, respectively (Scheme 1) [13,14], and in these and other papers [15,16], we showed some of the unusual chemistry enabled by the protic functionality, and the use of ^{15}N NMR chemical shifts in studying structure. Subsequent work by Hahn and Cossairt groups using 2-phosphinoethyl tethers has appeared; in particular, prolignands **3** and **4** lead to bis- and tris-PNHC species [17]. In 2008, the Ikariya group reported conversion of *N*-(pyrid-2-yl)benzimidazole to PNHC species **5** using tetramer $(\text{Cp}^*\text{RuCl})_4$ in refluxing THF [18]. In 2010, Song et al. managed to form a pyridylene PNHC complex **7** at ambient temperature, but needed the special rigidity of prolignand **6**, the ability of Ir(I) for metalation, and the stabilizing influence of NH–Cl hydrogen bonding to isolate solely the PNHC [19].



Scheme 1. Examples of prior tethered protic NHC (PNHC) and prolignands, and the present work on **8** and **9**.

Here, we extend this one-pot metalation chemistry to a homologous pair of pyrid-2-yl and even more conformationally flexible pyrid-2-ylmethyl 4-*tert*-butylimidazoles **3a** and **3b**, using both Cp^*Ir and Cp^*Rh fragments using $[\text{Cp}^*\text{M}^{\text{III}}\text{Cl}(\mu\text{-Cl})_2]$ and ionizing agents to make complexes of form **4**. Notably, the use of one equiv. of AgPF_6 per Cp^*MCl_2 unit allowed room temperature reaction conditions to succeed for all four ligand–metal combinations, suggesting general applicability or importance of ionization as a means of promoting PNHC formation from precursors with M–halide bonds.

2. Results

2.1. Syntheses and Characterization by NMR and X-ray Diffraction

Proligand **8a** was reported in 2010, made for another purpose, but only in 36% yield [20]. Our first attempt to improve the yield avoided the use of Cu(I) catalysis: a solution of *tert*-butylimidazole in *N*-methylpyrrolidinone (NMP) was treated with NaH to make the conjugate base sodium salt, and then 2-bromopyridine was added and the mixture heated. The likely mechanism for substitution involves rate-determining addition of imidazolate N to pyridine C2, disrupting aromaticity, followed by facile loss of bromide. Once the reaction was completed by heating to 100 °C for 17 h, removal of the NMP by vacuum distillation into a liquid nitrogen trap, followed by silica column chromatography of the residue, gave **8a** in improved but still moderate 59% yield.

We returned to Cu(I) catalysis, used DMF as lower-boiling solvent than NMP, and used a different base and higher reaction temperature and longer time (120 °C, 82 h). After reaction completion, workup as above and silica column chromatography yielded the product in a better yield of 70%.

Our first attempt to make novel **8b** proligand started with NaH in NMP used to generate *tert*-butylimidazolate sodium salt. The requisite (chloromethyl)pyridine was then added and the reaction mixture was allowed to warm up to room temperature, in which *tert*-butylimidazole anion presumably performed an S_N2 displacement on the (chloromethyl)pyridine electrophile. This reaction, unlike that for **8a**, occurred readily at room temperature. Removal of NMP was accomplished via vacuum distillation into a nitrogen trap, and silica column chromatography gave **8b** in a modest 48% yield.

An alternative method avoided the use of strong base and NMP. These adjustments made both the reaction preparation and purification **8b** more facile. Following a preparation seen in literature, for analogs lacking the *tert*-butyl group [21], *tert*-butylimidazole, potassium hydroxide, (chloromethyl)pyridine hydrochloride, and tetrahydrofuran were added to a round bottom flask fitted with a reflux condenser, and subsequently refluxed at 70 °C for 2–3 days. The higher temperature of the reaction allows for the usage of a weaker base for deprotonation and subsequent nucleophilic attack via a one-pot synthesis. Extraction of the products from the reaction mixture with dichloromethane and subsequent recrystallization of the solids obtained gave 86% yield.

Attempts to find a straightforward synthetic method for complexing **8a** and **8b** ligands proved to be more difficult than anticipated. Initially, [Cp*Ir^{III}Cl(μ-Cl)]₂ and **8b** were dissolved in 0.5 to 1 molar ratio in NMP and heated to 60 °C for 11 days, but no product was observed. In an attempt to lower the reaction temperature, KPF₆ was added to the reaction mixture to ionize chlorides and aid in the complexation of the ligands to the metal. The addition of KPF₆ led to complete complexation within 3 to 5 days but, in the case of forming **9b-Ir**, two products in a ratio of 9:1 were observed by ¹H NMR spectroscopy. The peaks for the major product were shadowed by smaller minor product peaks. Specifically, mutually coupled doublets for the diastereotopic methylene spacer protons of the major product appeared near 5.6 and 5.0 ppm, whereas the minor product peaks were seen at 5.8 and 4.9 ppm. The N–H peaks for the major and minor product occur were seen at 11.6 and 11.8 ppm respectively. Adding KPF₆ alleviated the need for high temperatures, but the difficulty of completely removing NMP spawned the continued search for better reaction conditions.

The use of KPF₆ in THF at 60 °C was carried out with both ligand precursors **8a** and **8b**, and with rhodium and iridium precursors, yielding **9a-Ir**, **9b-Ir**, **9a-Rh** and **9b-Rh**. All of the reactions required several days of heating at 60 °C in the low boiling solvent tetrahydrofuran. Only the iridium reaction with **8b** showed a second minor product, whereas the other three reactions appeared to contain only one product by NMR spectroscopic analysis. Early attempts used excesses of KPF₆, leading to crystallized products containing an extra hexafluorophosphate anion and potassium cation, as seen from a representative structure in Figure 1. By contrast, use of little more than one equivalent of KPF₆ per Ir or Rh allowed for isolation of bulk material with correct CHN analyses.

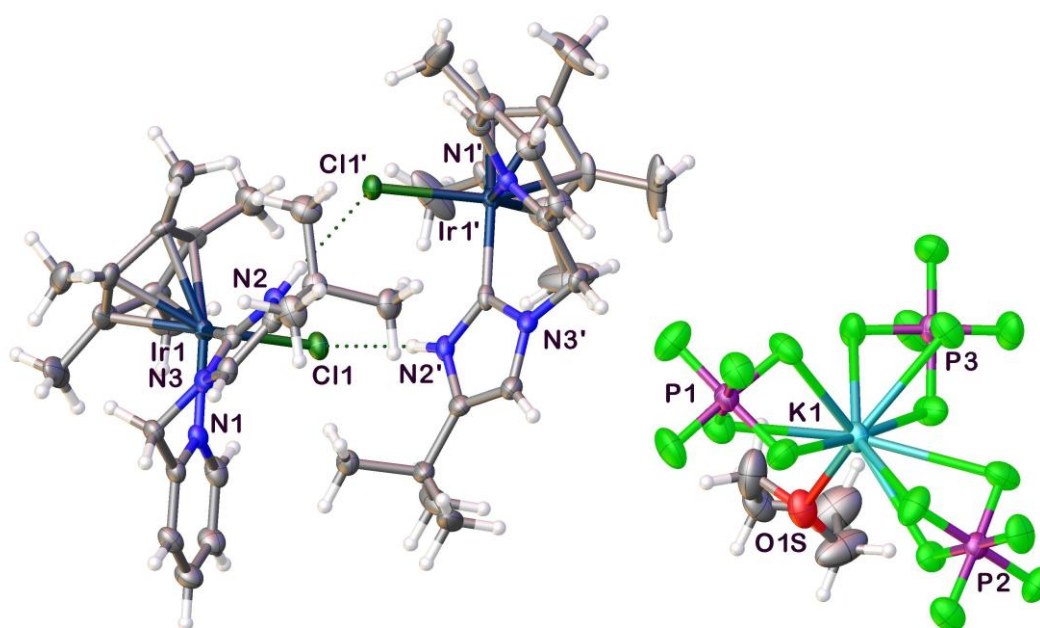
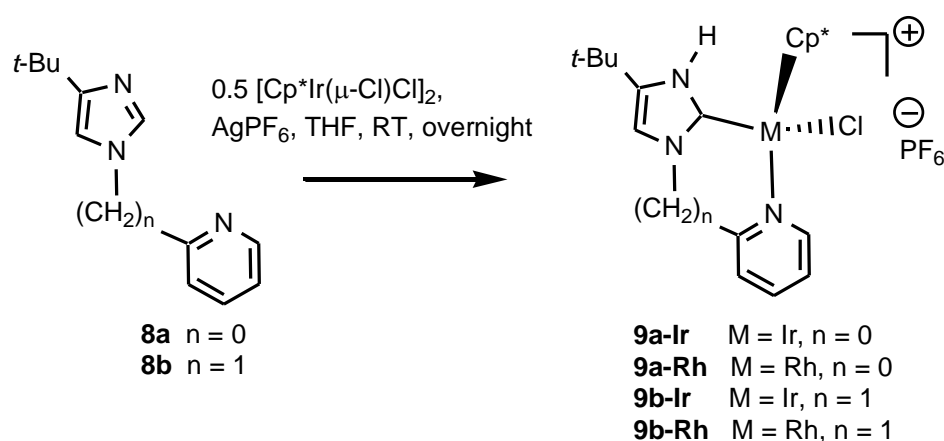


Figure 1. Crystal structure of **(9b-Ir)KPF₆·1.5THF** isolated using KPF₆ as described in the text. One THF molecule is excluded for clarity. The graphic shows bonds between K⁺ and three PF₆[−] ions but the structure should be regarded as ionic.

The final optimized procedure for synthesizing complexes **9a-Ir**, **9b-Ir**, **9a-Rh** and **9b-Rh** used silver hexafluorophosphate with the anticipation that the silver(I) cation would more efficiently ionize the chlorides and allow for easier binding of the proligand to the metal center (Scheme 2). To our delight, both ionization and subsequent formation of PNHC complexes occurred at room temperature. In addition, the crystallized products contained neither excess silver nor hexafluorophosphate as demonstrated by elemental analysis.



Scheme 2. Optimized room temperature formation of PNHC complexes of form **9** from **8a** and **8b**, using AgPF₆.

Unfortunately, the many attempts to form crystals of complexes derived from **8a** were unsuccessful. Fortunately, X-ray quality crystals for **9b-Ir** and **9b-Rh** were obtained and led to the structures seen below in Figures 2 and 3 respectively. CCDC 1814025-1814027 contains the supplementary crystallographic data for this paper (Supplementary Materials). These data can be

obtained free of charge via <http://www.ccdc.cam.ac.uk/conts/retrieving.html> (or from the CCDC, 12 Union Road, Cambridge CB2 1EZ, UK; Fax: +44-1223-336033; E-mail: deposit@ccdc.cam.ac.uk).

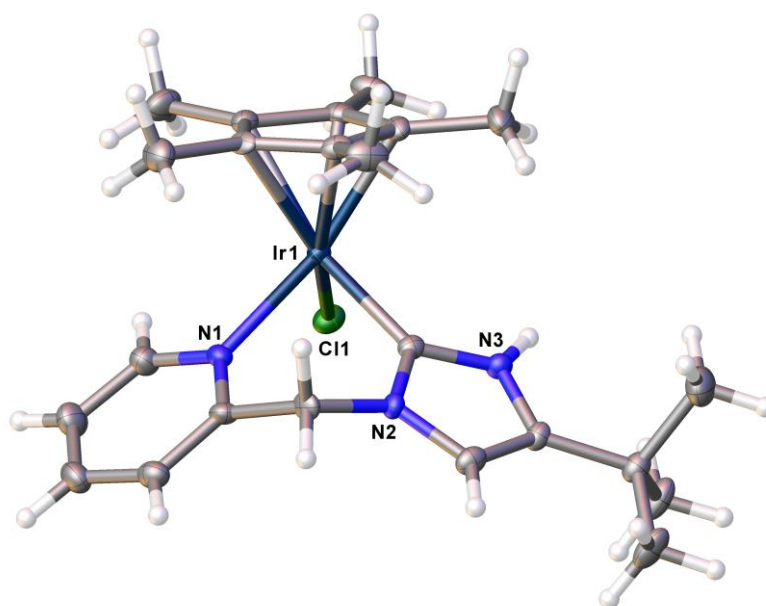


Figure 2. Crystal structure of the cation of **9b-Ir**; PF_6^- anion and two THF molecules are excluded for clarity.

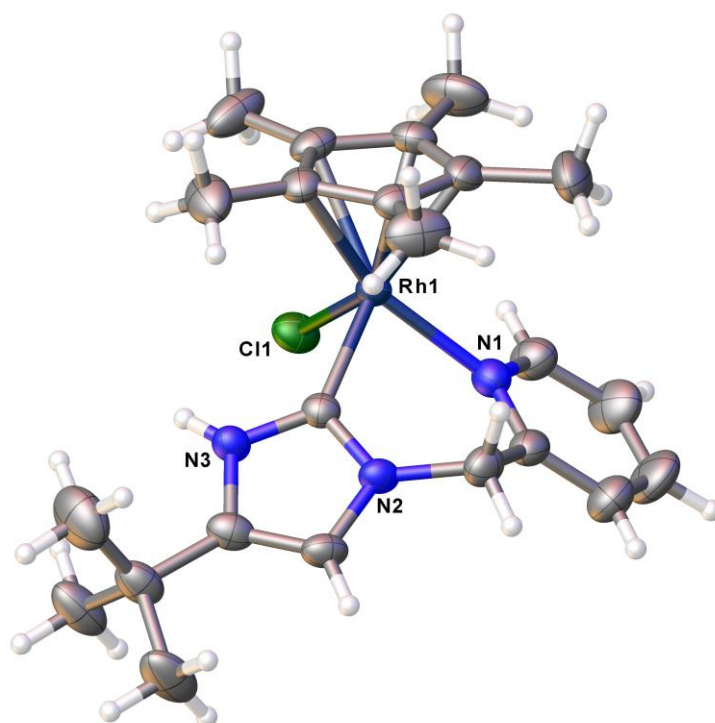


Figure 3. Crystal structure of the cation of **9b-Rh**; PF_6^- anion and two THF molecules are excluded for clarity.

The bond angles and distances for the cations of complexes **9b-Ir** and **9b-Rh** are similar in both the iridium and rhodium analogues, as seen in Table 1. In fact, bond distances are essentially identical within experimental uncertainty. Both structures are octahedral, with Cp^* occupying three facial sites.

The Cl1–M1–C1 bond angles for both the iridium and rhodium analogues are around 90°, and in both cases, the NH is pointed away from the chloride.

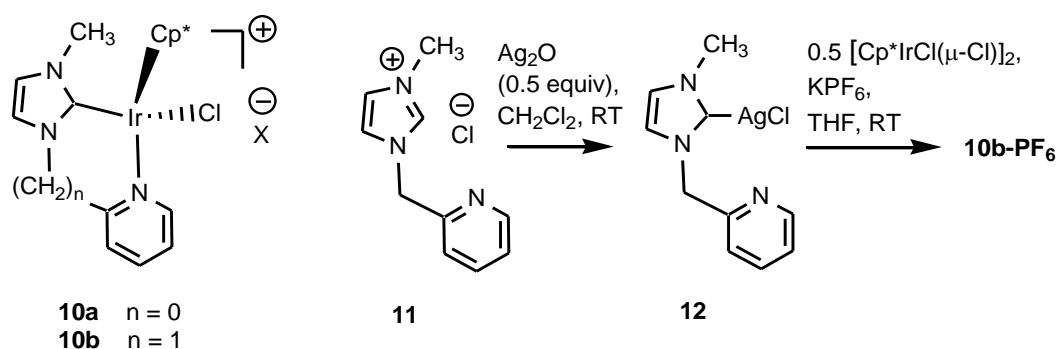
Table 1. Selected bond distances (Å) and angles (°) in the cations of **9b-Ir** and **9b-Rh**.

Bond	9b-Ir	9b-Rh	Angles	9b-Ir	9b-Rh
M1–C1	2.017(3)	2.020(4)	Cl1–M1–C1	89.33(11)	90.66(12)
H1N–C1	3.436	3.432	Cl1–M1–N3	86.46(9)	88.08(11)
M1–N3	2.108(2)	2.111(4)	C1–Ir1–N3	85.01(12)	85.49(16)
C11–M1	2.4154(8)	2.407(1)	-	-	-

The Ir–carbene and Ir–pyridine distances, and carbene–Ir–pyridine angle are also almost identical to those reported by Xiao et al. [22] for the cation of *N*-methylated analog of **9b-Ir**, NHC complex **10b** (Scheme 3). Those literature data are Ir–C 2.022(14) and Ir–N 2.097(10) Å, and angle 85.4(5)°.

By analogy, we suggest that the angles and bond distances of the **4a-Ir** and **4a-Rh** are very similar to one another, and also very similar to those reported for the *N*-methylated analog **10a**.

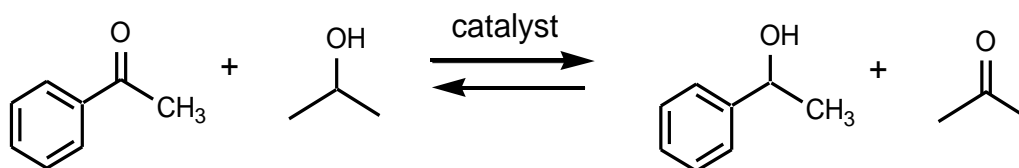
To help assess the role of the NH group, we prepared standard NHC complex **10b-PF₆** (X = PF₆) (Scheme 3). The imidazolium salt **11** was converted to **12**, followed by transmetalation using [Cp*Ir^{III}Cl(μ-Cl)]₂ in the presence of KPF₆.



Scheme 3. Related NHC complexes with *N*-methyl group. In this work, **10b-PF₆** (X = PF₆) was made by the route shown; previously, Xiao et al. had made **10a-Cl** and **10b-Cl** and **10b-(Cp*IrCl₃)**.

2.2. Catalysis

We compared our catalysts in transfer hydrogenation reactions following protocols found in literature [23,24]. We focused on the reduction of acetophenone to 1-phenylethanol using potassium hydroxide (0.1 equiv.) as base and 1 mol % catalyst loadings, as seen in Scheme 4. Because this process generates a chiral compound, and the Cp*M-containing catalysts are all chiral (but made here in racemic form), eventually, in future work, one might envision making enantiopure versions of the catalysts and studying enantioselective reductions.



Scheme 4. Transfer hydrogenation used to evaluate catalysts in this work.

Reactions were carried out air-free in dried 20 mL scintillation vials, and in the glovebox. Aliquots from each reaction were removed at 1 h, 3 h, 6 h, 20 h, 2 days, and 3 days time intervals. In cases

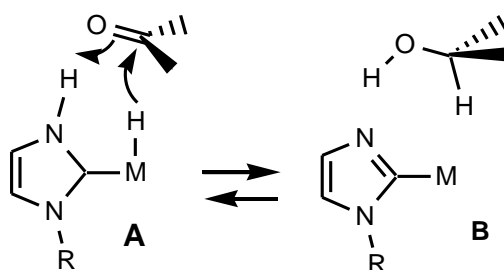
where catalysis was complete in less than one hour, aliquots were taken every 5 min. All yields are calculated via ^1H NMR integrations of the peaks for the product and remaining reactants using an inert internal standard (1,3,5-trimethoxybenzene), which has been used elsewhere [23]. The molar ratio of isopropanol (reductant) to acetophenone (substrate) was 20 to 1. We searched for a literature determination of K_{eq} for the reaction in Scheme 4, but were surprised not to find a value. Assuming K_{eq} is 1, the maximum yield of reduction product expected would be 95%. The percent yields in Tables 2 and 3 are given to the nearest 0.1, but the estimated uncertainty of NMR integrations is in the order of 1–2%; because one compares integrals of standard and analyte, the uncertainties in the yields reported are conservatively estimated as about 3%.

Table 2. Yields (%) of product over time (h) using **9a-Ir**, **9b-Ir**, **10b-PF₆**, or $[\text{Cp}^*\text{Ir}^{\text{III}}\text{Cl}(\mu\text{-Cl})_2]$ [a].

Time (h)	$[\text{Cp}^*\text{Ir}^{\text{III}}\text{Cl}(\mu\text{-Cl})_2]$	9a-Ir	9b-Ir	10b-PF₆
0	0	0	0	0
1	58.7	11.0	36.9	2.7
3	66.2	34.9	75.4	7.6
6	66.6			15.7
20	91.2			36.1
48	80.8			54.2
72	80.7			61.3

[a] Using 1 mol % catalyst (0.5 mol % of dimer $[\text{Cp}^*\text{Ir}^{\text{III}}\text{Cl}(\mu\text{-Cl})_2]$), 0.1 equiv. KOH, *i*-PrOH solvent, 82 °C.

As seen in the results found in Table 2, the methylene spacer-containing complex **9b-Ir** is three times faster than its homolog **9a-Ir** lacking the spacer. Although exact bond distances and angles cannot be directly compared due to the lack of crystal structure for **9a-Ir**, one can extrapolate based on the data from the literature NHC complexes **10a** and **10b**. If Scheme 5 applies, the methylene spacer may serve to decrease the distance between the ketone substrate and the N–H, leading to faster reduction. Also Scheme 5 may explain why *N*-methylated complex **10b-PF₆** is approximately 10 times slower than the PNHC analog **4b-Ir**. See Discussion for more details.



Scheme 5. Suggested mechanism of transfer hydrogenation reactions involving PNHC complexes.

$[\text{Cp}^*\text{Ir}^{\text{III}}\text{Cl}(\mu\text{-Cl})_2]$ was also used as catalyst, and in fact, was initially faster than **9a-Ir** and **9b-Ir**. A number of $[\text{Cp}^*\text{Ir}^{\text{III}}\text{Cl}(\mu\text{-Cl})_2]$ -derived catalysts contain NHC or phosphine ligands, and in some cases, the simple parent complex $[\text{Cp}^*\text{Ir}^{\text{III}}\text{Cl}(\mu\text{-Cl})_2]$ is indeed superior. Unfortunately, not all publications bother to include control experiments with $[\text{Cp}^*\text{Ir}^{\text{III}}\text{Cl}(\mu\text{-Cl})_2]$, as we have done here.

As for the Ir complexes, **9b-Rh** with methylene spacer was faster than **9a-Rh**: **9b-Rh** was 6 times faster than **9a-Rh**, as defined by comparing the times needed for 50% conversion of product (Table 3, ca. 60 min versus 10 min). Also of interest is the fact that the rhodium PNHC complexes were much faster than their iridium counterparts (Table 2 vs. Table 3). Given the estimated 3% uncertainty in yield values discussed above, we could say that **9b-Rh** achieves theoretical ca. 95% yield at 30–45 min, whereas **9a-Rh** requires almost 6 times longer (3 h), and the Ir complexes do not achieve theoretical yields under the conditions we have examined.

Table 3. Yields (%) of product over time (min) using **9a-Rh**, **9b-Rh**, or $[\text{Cp}^*\text{Rh}^{\text{III}}\text{Cl}(\mu\text{-Cl})_2]$ [a].

Time (min)	9a-Rh	9b-Rh	$[\text{Cp}^*\text{Rh}^{\text{III}}\text{Cl}(\mu\text{-Cl})_2]$
0	0	0	0
5	13.9	19.8	2.5
10	-	54.8	4.0
15	18.4	73.8	3.8
20	-	84.5	4.1
25	22.9	92.0	4.2
30	-	92.7	4.5
35	24.7	95.4	4.3
40	-	92.1	5.1
45	32.4	94.5	5.5
50	-	91.6	5.8
55	-	97.0	5.0
60	49.1	96.3	5.7
180	99.7	94.8	9.5

[a] Using 1 mol % catalyst (0.5 mol % of dimer $[\text{Cp}^*\text{Rh}^{\text{III}}\text{Cl}(\mu\text{-Cl})_2]$), 0.1 equiv. KOH, *i*-PrOH solvent, 82 °C.

3. Discussion

In forming PNHC complexes from proligands **8a** and **8b**, the pyridyl and pyridylmethyl tethers were successfully used in conjunction with a *tert*-butyl group that effectively blocks coordination of the metal to the imidazole nitrogen. Use of KPF_6 as ionizing agent speeds up metalations considerably, but heating at 60 °C for some days was still required, whether the solvent used was THF for the syntheses reported, or the more polar NMP. More dramatic was the ability to use ambient temperatures for metalation in less than 24 h, when AgPF_6 was employed. These results may inform future work on forming PNHC complexes from neutral imidazole or pyridine precursors by one-pot direct functionalization of a CH bond.

Turning to catalysis by Ir complexes, N-CH_3 species **10b-PF₆** was about 10× slower than its PNHC counterpart, **9b-Ir**, consistent with Scheme 5. Also consistent with Scheme 5 is the fact that in both the Ir and Rh series, the methylene spacer led to faster reactions (ca. 3× for Ir, 6× for Rh). The distance between NH and MH would be less in the complexes with methylene spacers, allowing better interaction with the C=O of substrate. An indication can be had by looking at published crystal structures of complexes **10a-Cl** and **10b-(Cp*IrCl₃)** [22]. The distance between the carbon of the N-CH₃ and the chlorine of the M-Cl units is 4.32 Å for **10a-Cl** and 3.48 Å for **10b-(Cp*IrCl₃)**. The more rigid ligand in **9a** and **10a** holds the NH quite far from the secondary sphere of the metal. Further significant effort will be needed to study the mechanism in detail.

Of all the catalysts examined, **9b-Rh** was the fastest, being about 6 times faster than either its Ir congener or the Rh homolog **9a-Rh**.

The rates of catalysis by the CpIr^* species here are in the range of rates reported for a variety of Cp^*Ir complexes, where temperatures of about 80 °C are used, often with co-catalytic base (recent examples: [25,26]). As a side note, to achieve faster rates, e.g., activity at ambient temperature, it would appear that a mono-dentate NHC is needed on Cp^*Ir [27]. For a particularly thorough comparison paper, see work of Hintermair et al. [24]; first, they actually include $[\text{Cp}^*\text{Ir}^{\text{III}}\text{Cl}(\mu\text{-Cl})_2]$, which is a rather good catalyst (60% in their work and 66% in ours, under identical conditions). Hintermair et al. tested 14 different molecular catalysts, but only two of the species achieved >95% yield after 3 h. To our knowledge, a similarly thorough comparison of Cp^*Rh species has not appeared. Notable in our work is the **9b-Rh** obtained at 95% yield in less than an hour. The faster catalysis by the Rh species may be a result of the trend that second row transition metals typically form weaker metal ligand bonds than third row metals, leading to more facile turnover during catalysis.

The ability of XH/MH systems (X = O or N) to facilitate a variety of reactions remains a very active area of research (examples: [28,29]), and further exploration of systems like the one here is definitely warranted.

4. Materials and Methods

For general experimental conditions, see other articles from our lab, for example [16,30,31].

4.1. Synthesis of **8a** Using NaH

In the glovebox, sodium hydride (60% in mineral oil) (0.6470 g, 0.01617 mol) was added to an oven-dried 50 mL Schlenk flask, and washed with hexane (2×5 mL). Each time the mixture was stirred, and then allowed to settle, followed by removal of the solvent wash via pipet. The washed sodium hydride was placed under Teflon pump vacuum until dry, and then suspended in *N*-methylpyrrolidinone (3 mL). *tert*-Butylimidazole (2.0055 g, 0.01617 mol) in *N*-methylpyrrolidinone (7 mL) was added dropwise to the Schlenk flask and allowed to stir, and vented while bubbling occurred. After the reaction mixture stopped bubbling and cleared, it was placed under nitrogen outside the glovebox and the flask placed in an ice bath. Using a syringe, 2-chloropyridine (1.517 mL, 0.01616 mol) was added to the cooled Schlenk flask. The reaction mixture turned orange, and the flask was allowed to warm to ambient temperature. The reaction mixture was then placed in a 100 °C oil bath and allowed to stir for 17 h. Reaction completion was monitored by the analysis of an aliquot by ^1H NMR spectroscopy (Varian, Palo Alto, CA, USA). After the removing the reaction from the oil bath, deionized water (5 mL) was added to the mixture. The *N*-methylpyrrolidinone and water were removed via vacuum distillation with heating by a heat gun and trapping of the solvent in a liquid nitrogen cold trap, leaving behind a red solid. The red solid was mixed with water (70 mL), and product was extracted with (6×50 mL) dichloromethane. The organic layers were combined and dried with sodium sulfate. The dried organic layers were filtered through a coarse fritted funnel and concentrated via rotary evaporation. The yellow oil was then dried to completion on a Schlenk vacuum line. The identity of the resulting yellow oil (1.9289 g, 59% yield) was confirmed by ^1H and ^{13}C NMR spectroscopy. ^1H NMR (chloroform- d_1 , 400 MHz, 30 °C) δ 8.46 (ddd, $J = 0.8, 1.9, 4.8$ Hz, 1 H), 8.32 (s, 1 H), 7.94 (ddd, $J = 1.3, 6.9, 8.8$ Hz, 1 H), 7.67 (td, $J = 0.9, 8.2$ Hz, 1 H), 7.54 (d, $J = 1.7$ Hz, 1 H), 7.29 (ddd, $J = 0.9, 4.9, 7.4$ Hz, 1 H), 1.30 (s, 9 H). ^{13}C NMR (chloroform- d_1 , 100 MHz, 30 °C) δ 154.6, 150.5, 149.9, 140.2, 134.5, 122.5, 113.0, 110.4, 30.4, 30.7. Anal. Calcd. for $\text{C}_{12}\text{H}_{15}\text{N}$ (201.13): C, 71.61; H, 7.51; N, 20.88. Found C, 71.33; H, 7.90; N, 20.67.

4.2. Synthesis of **8a** [2-(4-*tert*-butyl-1H-imidazol-1-yl)pyridine] Using CuI

In the glovebox, dimethylformamide (2 mL) was added to a 50 mL oven-dried Schlenk flask containing copper (I) iodide (0.0401 g, 0.211 mmol), *tert*-butylimidazole (0.1239 g, 0.998 mmol), and Cs_2CO_3 (0.06938 g, 0.2129 mmol). The reaction flask was removed from the glovebox and the contents put under an N_2 atmosphere. A syringe was used to add 2-bromopyridine (0.1000 mL, 1.025 mmol) to the Schlenk flask, and the reaction mixture and was allowed to stir at ambient temperature for 45 min. The reaction mixture was then placed in a 120 °C oil bath and allowed to stir for 82 h. After cooling to ambient temperature, ethyl acetate (10 mL) was added to the reaction mixture. The resulting reddish solution was loaded onto a silica plug and product was eluted with ethyl acetate (2×100 mL). The cloudy eluant was filtered through Celite, and the filtrate was concentrated by rotary evaporation, and the residue stored under oil pump vacuum. The resulting reddish oil was loaded onto a silica column and eluted with ethyl acetate. The product containing fractions were combined, dried with magnesium sulfate, filtered, and the filtrate concentrated by rotary evaporation. The identity and purity of the yellow oil (0.1406 g, 70% yield) was confirmed by ^1H and ^{13}C NMR.

4.3. Synthesis of **9a-Ir** with the Aid of KPF_6

Dry, deoxygenated tetrahydrofuran (4 mL) was added to a 20 mL scintillation vial containing **8a** (0.1531 g, 0.7606 mmol, 2.077 equiv.), $[Cp^*Ir^{III}Cl(\mu-Cl)]_2$ (0.2917 g, 0.3661 mmol), and KPF_6 (0.1445 g, 0.7850 mmol, 2.14 equiv.). The vial containing the orange heterogenous reaction was then placed in a 60 °C oil bath and allowed to stir for 44 h. The yellow reaction mixture was concentrated under Teflon pump vacuum. The remaining yellow solid was resuspended in deoxygenated acetone (2 mL) and filtered through a Celite plug to remove KCl precipitate. The Celite plug was washed with deoxygenated acetone (3 × 3 mL), and the filtrate was collected in a tared vial and concentrated under Teflon pump vacuum. Pentane (2 × 20 mL) was added to the solid and then concentrated under Teflon pump vacuum after each addition of pentane. The resulting yellow solid (0.4645 g, 86.1% yield) was confirmed as **9a-Ir** by 1H NMR and ^{13}C NMR spectroscopy. 1H NMR (acetone- d_6 , 600 MHz, 30 °C) δ 12.18 (bs, 1 H), 8.80 (ddd, $J = 0.8, 1.4, 7.6$ Hz, 1 H), 8.28 (dt, $J = 1.8, 6.5$ Hz, 1 H), 8.20 (ddd, $J = 0.8, 1.3, 8.3$ Hz, 1 H), 8.03 (s, 1H), 7.60 (dt, $J = 1.3, 8.5$ Hz, 1 H), 1.86 (s, 15 H), 1.43 (s, 9 H). ^{13}C NMR (acetone- d_6 , 600 MHz, 30 °C) δ 167.82, 153.40, 152.55, 147.12, 143.01, 124.91, 113.01, 111.63, 93.43, 31.92, 28.27, 8.23. Anal. Calcd. for $C_{22}H_{30}ClF_6N_3PIr$ (709.13): C, 37.26; H, 4.20; N, 5.93. Found: C, 37.73; H, 4.53; N, 6.11.

4.4. Synthesis of **9a-Ir** with the Aid of $AgPF_6$

Dry, deoxygenated tetrahydrofuran (4.5 mL) was added to a 20 mL scintillation vial containing **8a** (0.0317 g, 0.157 mmol, 1.98 equiv.), $[Cp^*Ir^{III}Cl(\mu-Cl)]_2$ (0.0631 g, 0.0792 mmol), and $AgPF_6$ (0.0474 g, 0.187 mmol). The reaction vial containing the orange heterogenous solution was covered with aluminum foil and allowed to stir for 22 h at room temperature. The reaction mixture solution was filtered through a Celite plug to remove $AgCl$ precipitate. The Celite plug was washed with deoxygenated THF (3 × 3 mL), and the filtrate was collected in a tared vial and concentrated under Teflon pump vacuum. Pentane (2 × 5 mL) was added to the solid, and then concentrated under Teflon pump vacuum after each addition of pentane. The resulting yellow solid (0.0927 g, 83% yield) was confirmed by 1H NMR and ^{13}C NMR spectroscopy.

4.5. Synthesis of **9a-Rh** with the Aid of KPF_6

Dry, deoxygenated tetrahydrofuran (1.5 mL) was added to a 20 mL scintillation vial containing **8a** (0.0750 g, 0.372 mmol, 2.07 equiv.), $[Cp^*Rh^{III}Cl(\mu-Cl)]_2$ (0.1106 g, 0.1789 mmol), and KPF_6 (0.0696 g, 0.378 mmol, 2.11 equiv.). The red/brown heterogenous reaction was then placed in a 60 °C oil bath and allowed to stir for 10 d. The orange reaction mixture was concentrated on Teflon pump vacuum. The remaining yellow solid was resuspended in deoxygenated acetone (2 mL), and filtered through a Celite plug to remove KCl precipitate. The Celite plug was washed with deoxygenated acetone (3 × 3 mL), and the filtrate was collected in a tared vial and concentrated under Teflon pump vacuum. Pentane (2 × 20 mL) was added to the solid and then concentrated with a Teflon pump vacuum after each addition of pentane. The resulting orange solid (0.1849 g, 80% yield) was confirmed as product by 1H , ^{31}P , and ^{13}C NMR spectroscopy. 1H NMR (acetone- d_6 , 400 MHz, 30 °C) δ 12.75 (bs, 1 H), 8.82 (td, $J = 0.7, 5.9$ Hz, 1 H), 8.29 (dt, $J = 1.6, 68.0$ Hz, 1 H), 8.13 (d, $J = 8.0$ Hz, 1 H), 8.05 (s, 1 H), 7.65 (dt, $J = 1.3, 6.3$ Hz, 1 H), 1.83 (s, 15 H), 1.44 (s, 9 H). ^{13}C NMR (acetone- d_6 , 100MHz, 30 °C) δ 180.49 (d, 51.6 Hz), 151.38, 151.313, 146.92, 141.88, 123.76, 112.47, 111.09, 99.22 (d, 6.7 Hz), 30.98, 28.34, 8.52. ^{31}P NMR (acetone- d_6 , 400 MHz, 30 °C) δ -144.260 (septet, $J = 707.2$ Hz). ^{19}F NMR (acetone- d_6 , 400 MHz, 30 °C) δ -75.66 (d, $J = 713.1$ Hz) Anal. Calcd. for $C_{22}H_{30}ClF_6N_3PRh$ (619.82): C, 42.63; H, 4.88; N, 6.78. Found: C, 43.10; H, 4.61; N, 7.15.

4.6. Synthesis of **9a-Rh** with the Aid of $AgPF_6$

Dry, deoxygenated tetrahydrofuran (4.5 mL) was added to a 20 mL scintillation vial containing **8a** (0.0307 g, 0.153 mmol), $[Cp^*Rh^{III}Cl(\mu-Cl)]_2$ (0.0488 g, 0.0789 mmol), and $AgPF_6$ (0.0402 g, 0.1590 mmol). The reaction vial containing the reddish heterogenous solution was covered with aluminum foil and

allowed to stir for 40 h at room temperature. The reaction mixture solution was filtered through a Celite plug to remove AgCl precipitate. The Celite plug was washed with deoxygenated THF (3 × 3 mL) and the filtrate was collected in a tared vial and concentrated with the Teflon high vacuum. The obtained solid was rinsed with pentane (2 × 5 mL), and solvent was removed by a Teflon pump vacuum after each addition of pentane. The resulting yellow solid (0.0927 g, 83% yield) was confirmed to be product by ^1H , ^{31}P , and ^{13}C NMR spectroscopy.

4.7. Synthesis of **9b-Ir** with the Aid of KPF_6

Dry, deoxygenated tetrahydrofuran (0.5 mL) was added to a 20 mL scintillation vial containing **8b** (0.0304 g, 0.141 mmol, 2.07 equiv.), $[\text{Cp}^*\text{Ir}^{\text{III}}\text{Cl}(\mu\text{-Cl})_2]$ (0.0543 g, 0.0681 mmol), and KPF_6 (0.0272 g, 0.147 mmol). The orange heterogeneous reaction was then placed in a 60 °C oil bath and allowed to stir for 5 d. The bright yellow reaction mixture was concentrated on a Teflon vacuum pump. The remaining orange solid was resuspended in deoxygenated acetone (2 mL) and filtered through a Celite plug to remove KCl precipitate. The Celite plug was washed with deoxygenated acetone (3 × 3 mL) and the filtrates were collected in a tared vial and concentrated with the Teflon vacuum pump. The resulting yellow solid **9b-Ir** (0.0884 g, 86% yield) was confirmed by ^1H , ^{13}C , ^{31}P , and ^{19}F NMR spectroscopy. ^1H NMR (acetone- d_6 , 400 MHz, 30 °C) δ 11.67 (s, 1 H), 8.96 (dd, $J = 1.2, 5.4$ Hz, 1 H), 8.11 (dt, $J = 1.5, 7.8$ Hz, 1 H), 7.83 (d, $J = 7.2$ Hz, 1 H), 7.59 (t, $J = 7.2$ Hz, 1 H), 7.23 (d, $J = 2.0$ Hz, 1 H), 1.74 (s, 15 H), 1.33 (s, 9 H). ^{13}C NMR (chloroform- d_1 , 100 MHz, 30 °C) δ 157.36, 140.22, 126.59, 125.32, 115.82, 53.76, 28.50, 8.26. ^{31}P NMR (acetone- d_6 , 400 MHz, 30 °C) δ -144.22 (septet, $J = 707.4$ Hz). ^{19}F NMR (acetone- d_6 , 400 MHz, 30 °C) δ -72.4 (d, $J = 707.4$ Hz). X-ray crystals were obtained by evaporative recrystallization from THF. Anal. Calcd. For $\text{C}_{23}\text{H}_{32}\text{ClF}_6\text{N}_3\text{PIr}$ (723.15): C, 38.20; H, 4.46; N, 5.81. Found: C, 38.93; H, 4.02; N, 5.55.

4.8. Synthesis of **9b-Ir** with the Aid of AgPF_6

In the glovebox, dry, deoxygenated tetrahydrofuran (1.5 mL) was added to a 20 mL scintillation vial containing **8b** (0.0107 g, 0.0497 mmol, 1.98 equiv.), $[\text{Cp}^*\text{Ir}^{\text{III}}\text{Cl}(\mu\text{-Cl})_2]$ (0.0200 g, 0.251 mmol), and AgPF_6 (0.0127 g, 0.0464 mmol). The reaction vial was covered with aluminum foil and allowed to stir for 17 h at room temperature. The bright yellow reaction mixture was concentrated using a Teflon pump vacuum. Pentane (2 × 20 mL) was added to the solid and then concentrated with a Teflon pump vacuum after each addition of pentane. The remaining yellow solid was resuspended in deoxygenated acetone (2 mL) and filtered through a Celite plug to remove AgCl precipitate. The Celite plug was washed with deoxygenated acetone (3 × 3 mL), and the filtrates were collected in a tared vial and concentrated under vacuum. The obtained solid was rinsed with pentane (2 × 20 mL), and solvent was removed under a Teflon pump vacuum after each addition of pentane. Yellow solid **9b-Ir** (0.0254 g, 70% yield) was obtained.

4.9. Synthesis of **9b-Rh** with the Aid of KPF_6

Dry, deoxygenated tetrahydrofuran (1 mL) was added to a 20 mL scintillation vial containing **8b** (0.0313 g, 0.145 mmol, 2.16 equiv.), $[\text{Cp}^*\text{Rh}^{\text{III}}\text{Cl}(\mu\text{-Cl})_2]$ (0.0418 g, 0.0676 mmol), and KPF_6 (0.0274 g, 0.148 mmol). The red/brown heterogeneous reaction was then placed in a 60 °C oil bath and allowed to stir for 4 days. The orange reaction mixture was concentrated on Teflon high vacuum. The remaining orange solid was redissolved in deoxygenated acetone (2 mL) and filtered through a Celite plug to remove KCl precipitate. The Celite plug was washed with deoxygenated acetone (3 × 3 mL), and the filtrate was collected in a tared vial and concentrated with the Teflon pump vacuum. Pentane (2 × 20 mL) was added to the solid and then concentrated with a Teflon pump vacuum after each addition of pentane. The resulting orange solid (0.0874 g, 95% yield) was confirmed as product by ^1H , ^{31}P , and ^{13}C NMR spectroscopy. ^1H NMR (acetone- d_6 , 400 MHz, 30 °C) δ 11.77 (s, 1 H), 8.99 (dd, $J = 1.3, 5.7$ Hz, 1 H), 8.11 (dt, $J = 1.5, 7.7$ Hz, 1 H), 7.78 (d, $J = 7.3$ Hz, 1 H), 7.62 (t, $J = 5.4$ Hz, 1 H), 7.29 (d, $J = 1.7$ Hz, 1 H), 5.64 (d, $J = 16.1$ Hz, 1 H), 5.15 (d, $J = 16.1$ Hz, 1 H), 1.72 (s, 15 H), 1.29 (s, 9 H).

^{13}C NMR (chloroform- d_1 , 100 MHz, 30 °C) δ 170.72 (d, $J_{\text{CRh}} = 50.4$ Hz), 156.51 (d, $^2J = 1.3$ Hz), 155.55, 144.76, 139.98, 125.89, 125.52, 117.02, 98.13 (d, $^1J_{\text{CRh}} = 6.4$ Hz), 30.61, 28.46, 8.59. ^{31}P NMR (acetone- d_6 , 400 MHz, 30 °C) δ -144.22 (septet, $J = 696.7$ Hz). ^{19}F NMR (acetone- d_6 , 400 MHz, 30 °C) δ -72.47 (d, $J = 707.5$ Hz). X-ray crystals were obtained by vapor diffusion of acetone and pentane. Anal. Calcd. for $\text{C}_{23}\text{H}_{32}\text{ClF}_6\text{N}_3\text{PRh}$ (633.84): C, 43.58; H, 5.09; N, 6.63. Found: C, 43.93; H, 4.71; N, 6.38.

4.10. Synthesis of **9b-Rh** with the Aid of AgPF_6

Dry, deoxygenated tetrahydrofuran (3 mL) was added to a 20 mL scintillation vial containing **8b** (0.0309 g, 0.143 mmol, 2.09 equiv.), $[\text{Cp}^*\text{Rh}^{\text{III}}\text{Cl}(\mu\text{-Cl})_2]$ (0.0423 g, 0.0684 mmol), and AgPF_6 (0.0367 g, 0.145 mmol). The reaction vial was covered with aluminum foil and allowed to stir for 34 h at room temperature. The orange reaction mixture was concentrated using a Teflon high vacuum. Pentane (2×20 mL) was added to the solid, and then concentrated with a Teflon pump vacuum after each addition of pentane. The remaining yellow solid was resuspended in deoxygenated acetone (2 mL), and filtered through a Celite plug to remove AgCl precipitate. The Celite plug was washed with deoxygenated acetone (3×3 mL), and the filtrate was collected in a tared vial and concentrated under Teflon pump vacuum. Pentane (2×20 mL) was added to the solid and then concentrated with a Teflon pump vacuum after each addition of pentane. The resulting orange solid (0.0741 g, 81% yield) was confirmed as product by ^1H , ^{31}P , and ^{13}C NMR spectroscopy.

4.11. Synthesis of **10b-PF₆**

In the glovebox, a vial was charged with solids $[\text{Cp}^*\text{Ir}^{\text{III}}\text{Cl}(\mu\text{-Cl})_2]$ (51.9 mg, 0.0651 mmol), silver carbene complex **12** (41.4 mg, 0.0652 mmol), and KPF_6 (23.9 mg, 0.1298 mmol). CH_2Cl_2 (3 mL) was added and the vial was capped, wrapped in foil, and the contents stirred for 3 days. The mixture was filtered through Celite and the filtrate evaporated. The crude product was dissolved in CH_2Cl_2 and pentane vapor was allowed to diffuse. The crystals were harvested, rinsed with CHCl_3 , and then dissolved in CH_2Cl_2 (ca. 10 mL) and the resulting solution passed through a small plug of silica, eluting with CH_2Cl_2 /acetone. The product so obtained (62.2 mg) was dissolved in acetone (5 mL) and ether vapor was allowed to diffuse. Yellow crystals (52.6 mg, 59%) of product were obtained. ^1H NMR (acetone- d_6 , 400 MHz, 30 °C) δ 8.98 (dd, $J = \sim 1, 5.5$ Hz, 1H), 8.13 (dt, $J = \sim 1, 7.6$ Hz, 1H), 7.85 (d, $J = 8.0$ Hz, 1H), 7.61 (dt, $J = \sim 1, 7.2$ Hz, 1H), 7.60 (d, $J = 2.0$, 1H), 7.49 (d, $J = 1.6$, 1H), 5.72 (d, $J = 16.0$ Hz, 1H), 5.06 (d, $J = 16.0$ Hz, 1H), 3.99 (s, 3H), 1.78 ppm (s, 15H). Anal. Calcd. for $\text{C}_{20}\text{H}_{26}\text{ClF}_6\text{IrN}_3\text{P}$ (681.11): C, 35.27; H, 3.85; N, 6.17. Found: C, 35.35; H, 3.67; N, 6.49.

4.12. General Catalytic Procedures for the Reduction of Acetophenone to 1-Phenylethanol

A stock reactant solution was made by mixing acetophenone (4.66 mL), isopropanol (60 mL), and 1,3,5-trimethoxybenzene (402.8 mg) as internal standard.

In the glovebox, finely ground potassium hydroxide (11.3 mg, 0.201 mmol) and **9b-Rh** (13.1 mg, 0.0206 mmol) were weighed into an oven-dried 20 mL scintillation vial. To the reaction flask was added the acetophenone/isopropanol (0.616 M) solution (3.25 mL, 2.00 mmol) containing trimethoxybenzene. The reaction vial was removed from the glovebox and placed in an 82 °C oil bath. The reaction flask was removed from the oil bath during specific time increments for removal of aliquots for analysis. Before aliquot removal, the reaction flask was cooled for 30 s in an ice bath, followed by being brought into the glovebox for removal of 0.2 mL of the reaction mixture. The aliquot was placed in an NMR tube. The aliquot was diluted with 0.5–1.0 mL of deuterated dichloromethane, and kept on ice until analysis by ^1H NMR spectroscopy.

9a-Rh (12.0 mg, 0.214 mmol), KOH (12.4 mg, 0.200 mmol), acetophenone/isopropanol solution (3.25 mL).

$[\text{Cp}^*\text{Rh}^{\text{III}}\text{Cl}(\mu\text{-Cl})_2]$ (6.1 mg, 0.0091 mmol), KOH (11.2 mg, 0.200 mmol), acetophenone/isopropanol solution (3.25 mL).

9b-Ir (15.5 mg, 0.0214 mmol), KOH (13.9 mg, 0.248 mmol), acetophenone/isopropanol solution (3.41 mL).

9a-Ir (14.9 mg, 0.0210 mmol), KOH (13.5 mg, 0.241 mmol), acetophenone/isopropanol solution (3.48 mL).

[Cp*Ir^{III}Cl(μ-Cl)]₂ (8.0 mg, 0.011 mmol), KOH (11.2 mg, 0.200 mmol), acetophenone/isopropanol solution (3.25 mL).

10b-PF₆ (13.6 mg, 0.0199 mmol), KOH (11.9 mg, 0.212 mmol), acetophenone/isopropanol solution (3.25 mL).

Supplementary Materials: The following are available online at <http://www.mdpi.com/2304-6740/6/1/27/s1>, cif and checkcif files for the structures (**9b-Ir**)KPF₆·1.5THF, **9b-Ir** and **9b-Rh**.

Acknowledgments: We thank LeRoy Lafferty, former head of the SDSU NMR Facility, for all of his help, and gratefully acknowledge partial financial support from the US National Science Foundation.

Author Contributions: Douglas B. Grotjahn and Jessica K. Martin conceived and designed the experiments and analyzed all but the X-ray diffraction data, Jessica K. Martin did most of the experiments, Taylon N. Tom made **10b-PF₆** and performed some catalysis experiments, Arnold L. Rheingold obtained and analyzed X-ray diffraction data, Jessica K. Martin wrote her thesis on her part of the work, Douglas B. Grotjahn wrote the paper.

Conflicts of Interest: The authors declare no conflict of interest.

References

1. Jahnke, M.C.; Hahn, F.E. Complexes with protic (NH,NH and NH,NR) *N*-heterocyclic carbene ligands. *Coord. Chem. Rev.* **2015**, *293–294*, 95–115. [[CrossRef](#)]
2. Kuwata, S.; Ikariya, T. Metal-ligand bifunctional reactivity and catalysis of protic *N*-heterocyclic carbene and pyrazole complexes featuring β-NH units. *Chem. Commun.* **2014**, *50*, 14290–14300. [[CrossRef](#)] [[PubMed](#)]
3. Huertos, M.A.; Perez, J.; Riera, L.; Menendez-Velazquez, A. From *N*-alkylimidazole ligands at a rhenium center: Ring opening or formation of NHC complexes. *J. Am. Chem. Soc.* **2008**, *130*, 13530–13531. [[CrossRef](#)] [[PubMed](#)]
4. Huertos, M.A.; Perez, J.; Riera, L.; Diaz, J.; Lopez, R. From bis(*N*-alkylimidazole) to bis(NH-NHC) in rhenium carbonyl complexes. *Angew. Chem. Int. Ed.* **2010**, *49*, 6409–6412. [[CrossRef](#)] [[PubMed](#)]
5. Ruiz, J.; Perandones, B.F. Base-promoted tautomerization of imidazole ligands to *N*-heterocyclic carbenes and subsequent transmetalation reaction. *J. Am. Chem. Soc.* **2007**, *129*, 9298–9299. [[CrossRef](#)] [[PubMed](#)]
6. Bonati, F.; Burini, A.; Pietroni, B.R.; Bovio, B. Reactions of *C*-imidazolyl lithium derivatives with group Ib compounds: Tris[μ-(1-alkylimidazolato-N³,C²)]trigold(I) and -silver(I). Crystal structure of bis(1-benzylimidazol-2-ylidene)gold(I) chloride. *J. Organomet. Chem.* **1989**, *375*, 147–160. [[CrossRef](#)]
7. Raubenheimer, H.G.; Cronje, S. Carbene complexes derived from lithiated heterocycles, mainly azoles, by transmetalation. *J. Organomet. Chem.* **2001**, *617–618*, 170–181. [[CrossRef](#)]
8. Meier, N.; Hahn, F.E.; Pape, T.; Siering, C.; Waldvogel, S.R. Molecular recognition utilizing complexes with NH,NH-stabilized carbene ligands. *Eur. J. Inorg. Chem.* **2007**, 1210–1214. [[CrossRef](#)]
9. Dobereiner, G.E.; Chamberlin, C.A.; Schley, N.D.; Crabtree, R.H. Acyl protection strategy for synthesis of a protic NHC complex via *N*-acyl methanolysis. *Organometallics* **2010**, *29*, 5728–5731. [[CrossRef](#)]
10. Isobe, K.; Kai, E.; Nakamura, Y.; Nishimoto, K.; Miwa, T.; Kawaguchi, S.; Kinoshita, K.; Nakatsu, K. *Trans*-bromo(2-, 3-, and 4-pyridyl)bis(triethylphosphine)palladium(II) complexes. *J. Am. Chem. Soc.* **1980**, *102*, 2475–2476. [[CrossRef](#)]
11. Isobe, K.; Kawaguchi, S. Organopalladium(II) complexes containing carbon-bonded pyridine and picoline as a ligand: Preparation, structures, and reactions. *Heterocycles* **1981**, *16*, 1603–1612.
12. Crociani, B.; Di Bianca, F.; Gioenco, A.; Scriveranti, A. Protonation and methylation reactions of 2-pyridyl-palladium(II) and platinum(II) complexes. *J. Organomet. Chem.* **1983**, *251*, 393–411. [[CrossRef](#)]
13. Miranda-Soto, V.; Grotjahn, D.B.; DiPasquale, A.G.; Rheingold, A.L. Imidazol-2-yl complexes of Cp*Ir as bifunctional ambident reactants. *J. Am. Chem. Soc.* **2008**, *130*, 13200–13201. [[CrossRef](#)] [[PubMed](#)]
14. Miranda-Soto, V.; Grotjahn, D.B.; Cooksy, A.L.; Golen, J.A.; Moore, C.E.; Rheingold, A.L. A labile and catalytically active imidazol-2-yl fragment system. *Angew. Chem. Int. Ed.* **2011**, *50*, 631–635. [[CrossRef](#)] [[PubMed](#)]

15. Marelius, D.C.; Moore, C.E.; Rheingold, A.L.; Grotjahn, D.B. Reactivity studies of pincer bis-protic *N*-heterocyclic carbene complexes of platinum and palladium under basic conditions. *Beilstein J. Org. Chem.* **2016**, *12*, 1334–1339. [[CrossRef](#)] [[PubMed](#)]
16. Marelius, D.C.; Darrow, E.H.; Moore, C.E.; Rheingold, A.L.; Grotjahn, D.B. Hydrogen-bonding pincers with two protic *N*-heterocyclic carbenes from direct metalation of a 1,8-bis(imidazol-1-yl)carbazole by platinum, palladium, as well as nickel. *Chem. Eur. J.* **2015**, *21*, 10988–10992. [[CrossRef](#)] [[PubMed](#)]
17. Flowers, S.E.; Cossairt, B.M. Mono- and dimetalation of a tridentate bisimidazole-phosphine ligand. *Organometallics* **2014**, *33*, 4341–4344. [[CrossRef](#)]
18. Araki, K.; Kuwata, S.; Ikariya, T. Isolation and interconversion of protic *N*-heterocyclic carbene and imidazolyl complexes: Application to catalytic dehydrative condensation of *N*-(2-pyridyl)benzimidazole and allyl alcohol. *Organometallics* **2008**, *27*, 2176–2178. [[CrossRef](#)]
19. Song, G.; Su, Y.; Periana, R.A.; Crabtree, R.H.; Han, K.; Zhang, H.; Li, X. Anion-exchange-triggered 1,3-shift of an NH proton to iridium in protic *N*-heterocyclic carbenes: Hydrogen-bonding and ion-pairing effects. *Angew. Chem., Int. Ed.* **2010**, *49*, 912–917. [[CrossRef](#)] [[PubMed](#)]
20. Peters, M.; Breinbauer, R. A simple synthesis of functionalized 3-methyl-1-pyridinyl-1H-imidazolium salts as bidentate *N*-heterocyclic-carbene precursors and their application in ir-catalyzed arene borylation. *Tetrahedron Lett.* **2010**, *51*, 6622–6625. [[CrossRef](#)]
21. Chiu, P.L.; Lai, C.-L.; Chang, C.-F.; Hu, C.-H.; Lee, H.M. Synthesis, structural characterization, computational study, and catalytic activity of metal complexes based on tetradentate pyridine/*N*-heterocyclic carbene ligand. *Organometallics* **2005**, *24*, 6169–6178. [[CrossRef](#)]
22. Xiao, X.-Q.; Jin, G.-X. Functionalized *N*-heterocyclic carbene iridium complexes: Synthesis, structure and addition polymerization of norbornene. *J. Organomet. Chem.* **2008**, *693*, 3363–3368. [[CrossRef](#)]
23. Gnanamgari, D.; Sauer, E.L.O.; Schley, N.D.; Butler, C.; Incarvito, C.D.; Crabtree, R.H. Iridium and ruthenium complexes with chelating *N*-heterocyclic carbenes: Efficient catalysts for transfer hydrogenation, β -alkylation of alcohols, and *N*-alkylation of amines. *Organometallics* **2009**, *28*, 321–325. [[CrossRef](#)]
24. Hintermair, U.; Campos, J.; Brewster, T.P.; Pratt, L.M.; Schley, N.D.; Crabtree, R.H. Hydrogen-transfer catalysis with Cp*Ir^{III} complexes: The influence of the ancillary ligands. *ACS Catal.* **2014**, *4*, 99–108. [[CrossRef](#)]
25. Navarro, M.; Smith, C.A.; Albrecht, M. Enhanced catalytic activity of iridium(III) complexes by facile modification of C,N-bidentate chelating pyridylideneamide ligands. *Inorg. Chem.* **2017**, *56*, 11688–11701. [[CrossRef](#)] [[PubMed](#)]
26. Mazloomi, Z.; Pretorius, R.; Pamies, O.; Albrecht, M.; Dieguez, M. Triazolylidene iridium complexes for highly efficient and versatile transfer hydrogenation of C=O, C=N, and C=C bonds and for acceptorless alcohol oxidation. *Inorg. Chem.* **2017**, *56*, 11282–11298. [[CrossRef](#)] [[PubMed](#)]
27. Corberán, R.; Peris, E. An unusual example of base-free catalyzed reduction of C=O and C=NR bonds by transfer hydrogenation and some useful implications. *Organometallics* **2008**, *27*, 1954–1958. [[CrossRef](#)]
28. Moore, C.M.; Szymczak, N.K. 6,6'-dihydroxy terpyridine: A proton-responsive bifunctional ligand and its application in catalytic transfer hydrogenation of ketones. *Chem. Commun.* **2013**, *49*, 400–402. [[CrossRef](#)] [[PubMed](#)]
29. Nieto, I.; Livings, M.S.; Sacci, J.B.; Reuther, L.E.; Zeller, M.; Papish, E.T. Transfer hydrogenation in water via a ruthenium catalyst with OH groups near the metal center on a bipy scaffold. *Organometallics* **2011**, *30*, 6339–6342. [[CrossRef](#)]
30. Larsen, C.R.; Erdogan, G.; Grotjahn, D.B. General catalyst control of the monoisomerization of 1-alkenes to *trans*-2-alkenes. *J. Am. Chem. Soc.* **2014**, *136*, 1226–1229. [[CrossRef](#)] [[PubMed](#)]
31. Grotjahn, D.B.; Kraus, J.E.; Amouri, H.; Rager, M.-N.; Cortes-Llamas, S.A.; Mallari, A.A.; DiPasquale, A.G.; Liable-Sands, L.M.; Golen, J.A.; Zakharov, L.N.; et al. Multimodal study of secondary interactions in Cp*Ir complexes of imidazolylphosphines bearing an NH group. *J. Am. Chem. Soc.* **2010**, *132*, 7919–7934. [[CrossRef](#)] [[PubMed](#)]

